MASTER PROJECT

High mountain streams could act as sources or sinks of CO_2 depending on watersheds characteristics

Author

Nicolas Manetti

Supervisors

Andrew Lean Robison

Nicola Deluigi

Professor

Tom Ian Battin

External Expert

Erin Hotchkiss

River Ecosystems Laboratory

School of Architecture, Civil and Environmental Engineering (ENAC)

Submitted

18.03.2022

Abstract

We studied twelve stream sites located in four watersheds in the Swiss Alps to examine CO_2 dynamics in high mountain streams. We observed interesting differences in median annual CO_2 flux, with some sites experiencing years of overall sink and others of overall source. Our study confirms pervious finding regarding glacier-fed streams being significant CO_2 sinks as a result of high rates of weathering within the catchment. However, our results show that the presence of a glacier is not necessary for a stream to be a sink of CO_2. We suggest that the balance of weathering to soil respiration across different type of catchments is a determining factor of whether a stream tends to either outgas or absorb CO_2.

Introduction

Inland waters are acknowledged as important components of the global carbon cycle, receiving and processing significant amounts of terrestrial carbon (Battin et al. 2009). More precisely streams and rivers play a central role in the global carbon cycle by transforming, outgassing and storing more than half of the carbon they receive from terrestrial ecosystems before delivery to the ocean (Drake et al. 2018). Therefore, ignoring inland waters in land carbon budgets may overestimate terrestrial carbon dioxide (CO_2) uptake and storage. There is consequently a fundamental need to understand the drivers and rates of carbon dynamics and transport in running waters.

The CO_2 found in stream waters is the result of the multiple recognized reactions and processes occurring in the streams themselves (internal) and in their watersheds (external), with some reactions result in production of CO_2, while others consume CO_2. Of the external processes, a major one is soil respiration, which defines the CO_2 produced by the biological activity in watershed soils and represents the most important pathway by which CO_2 fixed by photosynthesis returns to the atmosphere (Schlesinger and Andrews 2000). Weathering at the catchment scale is responsible for consumption of CO_2 through the dissolution of sediments and minerals, typically silicates and carbonates. Internal processes leading to CO_2 consumption include photosynthesis, which is responsible for carbon fixation by aquatic organisms capable of absorbing solar radiation and carbon, and calcite precipitation. Processing of dissolved organic carbon (DOC) is instead producing CO_2 in stream.

It has been observed that in most stream networks CO_2 producing reactions are dominant making most streams net sources of CO_2 to the atmosphere (Battin et al. 2009; Hotchkiss et al. 2015). Furthermore, the size of streams has been shown to be a core attribute to characterize CO_2 dynamics with headwater streams being prone to gather high amounts of terrestrially derived CO_2 and organics inputs, making them outgas more CO_2 compared to bigger rivers (Hotchkiss et al. 2015). Headwater streams represents the smallest parts of river and stream networks, but make up most of the river length, and are estimated to deliver more than 30% of the global water runoff (Meybeck et al. 2001).

Mountains are typical environments of headwater streams. Among landmass, mountainous landscapes compose 25% of the earth's land surface area and are estimated to deliver more than 30% of the global water runoff (Meybeck et al. 2001). Furthermore, headwater streams represent an important portion of inland waters and contribute to the emissions for 36% (i.e., 0.93 Pg C yr^{-1}) of total CO_2 outgassing from rivers and streams (Marx et al. 2017). However, most of our understanding of these environments is built around the investigation on headwater streams where CO_2 balances in stream water is dominated by soil respiration (Johnson et al. 2008; Wallin et al. 2013; Lauerwald et al. 2015). Soil development has been shown to be a key variable in the amount of terrestrially derived CO_2 and organic carbon inputs to the streams (Guelland et al. 2013). In soils, CO_2 effluxes has been shown to increase with site age, which was related to soil carbon accumulation and vegetation coverage. Nevertheless, many mountain catchments situated above the tree line are not characterized by important amount of soil development and supply of organic carbon. These environments have shown high temporal and spatial variability in CO_2 concentration and flux as a result of the influence of multiple factors such as solar radiation, seasonal melting of glaciers and snow, variations in precipitation, landscape characteristics and soil organic matter (Clow et al. 2021). St. Pierre et al. (2019) showed how glacier-fed freshwater ecosystems differ substantially from other mountain streams, with the potential to be significant sinks of CO_2. Watersheds with high glacier coverage exhibit high rates of weathering reactions, leading to the consumption of CO_2. Furthermore, high mountain streams with glaciated catchments are the type of environments with negligible inputs of soil carbon with poor soil development and carbon stock.

Another variable governing CO_2 concentrations and fluxes, particularly in high mountain streams, is discharge, which is a fundamental characteristic of streams and affects CO_2 effluxes and influxes in multiple ways. Firstly, as for any gas, CO_2 exchange across the air-water surface is influenced by flow regimes (Ulseth et al. 2019). Gas exchange, in fact, can be considerably higher in mountain streams because of the steeper landscapes typical of these freshwater ecosystems. Furthermore, discharge controls the dynamics and transport of sediments, weathering solutes, nutrients and dissolved organic carbon (DOC; Diamond and Cohen 2018). CO_2 does not differ in this regard and information on watershed characteristics and hydrology interactions can be drawn by exploring the responsiveness of CO_2 to discharge, in so-called concentration-discharge (C-q) relationships. Liu and Raymond (2018) showed that that CO_2 outgassing tends to increase with discharge, with small streams having the tendency to release higher amounts of CO_2 at higher discharge. The analysis of the relationship between CO_2 and stream specific discharge, in combination with other data about watershed structure and landscape characteristics, can be an useful way to gain mechanistic knowledge about CO_2 dynamics (Godsey et al. 2009).

In this study we characterized CO_2 exchange in high mountain streams to examine relationships between catchment characteristics and CO_2 concentration and emissions in streams. We analysed data covering four years of high-resolution sensor data to estimate CO_2 fluxes in twelve streams located in four distinct watersheds. This work allowed us to gain knowledge about high mountains stream CO_2 dynamics and gain interesting insight about how glacier coverage, soil development, and discharge affect CO_2 exchanges.

Methods

1.1 Site description

We studied twelve sites located in four watersheds in the Swiss Alps (Cantons of Valais and Vaud). The data used in this work were gathered in the context of the METALP project managed by the River Ecosystems Laboratory (RIVER) at the Ecole Polytechnique Fédérale de Lausanne (EPFL). These streams have been described in previous studies (e.g., Horgby et al. 2019; Ulseth et al. 2019; Canadell et al. 2021). The original design of METALP focused on understanding stream conditions and processes across altitudinal and glacial coverage gradients. The stations emplacements were chosen to explore these gradients both within catchments and between catchments, with three sites positioned in each of four larger watersheds. Sites were generally placed at upstream, downstream, and tributary sites in glacier fed systems. The watersheds are located in the Valsorey watershed which has a relatively large glacier, at an upstream (VAU), downstream (VAD), and tributary site (VEL); in Val Ferret with a relatively small glacier, with upstream (FEU), downstream (FED), and tributary (PEU) sites; in Vallon de Nant with downstream, AND, upstream ANU, and tributary RIC; in Champéry with upstream (VIU), middle (VIM) and downstream (VID) sites.

Figure 1: Locations of the 12 study sites (Horgby et al. 2019)

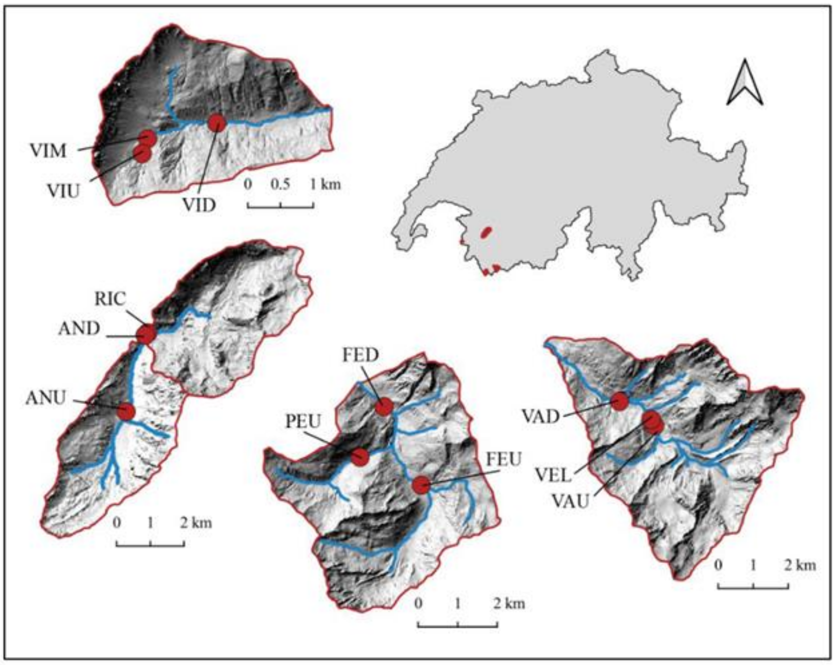

Briefly, seven streams are glacier fed (VAD, VAU, FED, FEU, AND, ANU, RIC) with glacial coverage ranging from 3.41% to 33.5% (Table 1). VAD and VAU presented largely the highest glaciated coverage with respectively 33.5% and 27.5%. The drainage areas varied from 0.31 km^2 (VIU) to 23.2 km^2 (VAD). Elevation was highest in Valsorey, and lowest in Champery with mean catchments altitude ranging from 1778 m at VID to 2893 m at VAU above sea level. Four streams drained partially forested catchments (VID, RIC, AND, ANU), the other eight are located above the tree line. Vegetation cover was typically highest in the low elevation catchments, with the highest being 94.0% at VID and lowest being 21.1% at VAU. From a geological standpoint, Champéry and Vallon de Nant watersheds are dominated by carbonate sedimentary rocks, whether Valsorey and Ferret are characterized by a metamorphic lithology (Horgby et al. 2019).

Table 1: Site characteristics, including watershed location, altitude, area, and land cover.

Catchment	Site	Station Altitude [m]	Area [km^2]	Glacier Coverage [%]	Vegetated Area [%]
Valsorey	VAD	1936	23.2	27.4	24.2
	VAU	2148	18.1	33.5	21.1
	VEL	2161	3.11	0	56.7
Ferret	FED	1773	20.2	3.41	62.4
	FEU	1996	9.33	7.40	46.3
	PEU	2024	3.97	0	70.2
Vallon de Nant	AND	1197	13.4	4.58	63.94
	ANU	1465	8.99	6.80	54.01
	RIC	1192	14.3	6.38	64.2
Champéry	VID	1416	3.64	0	94.0
	VIM	1630	0.74	0	86.1
	VIU	1689	0.31	0	80.9

1.2 Data collection

In each study site, high-frequency sensors measured water depth (mm; WT-HR 1000, Tru Track Ltd), dissolved CO_2 concentration (ppm, GMT220 probe sealed with PFTE membrane sleeve according to the procedure described in Johnson et al. 2010, Vaisala), water temperature and dissolved oxygen concentration (C° and mg O_2 L^{-1}; accuracy ± 5%, miniDOT, Precision Measurement Engineering). All parameters were recorded every 10 minutes when sensors were deployed and functioning. We analysed data collected from 2017 to 2020. The sites were visited approximately monthly for sensor maintenance and data downloading. Visits in winter were less frequent because of the presence of snow and risk of avalanche. Grab samples of water were collected during site visits and analysed for dissolved CO_2 concentration (ppm), dissolved organic carbon (DOC) concentration, and the isotopic composition of the dissolved inorganic carbon pool (δ^{13}C-DIC). All grab sample data is available on the METALP website (https://metalp.epfl.ch).

Discharge was calculated using rating curves from water depth , the development of which is described in Canadell et al. (2021).Barometric pressure was obtained from MeteoSwiss weather stations (network managed by the Swiss Federal Office and Meteorology and Climatology). The Col du Grand St Bernard station (elevation 2473 m) was used for the Valsorey and Ferret catchments, the Evionnaz station (482 m) for Champéry, and Les Diablerets (2964 m) station for Vallon de Nant. Barometric pressure (P, mbar) was adjusted for site-specific elevation and temperature following:

$$P = P_0 \exp\left(\frac{-gM(h-h_0)}{RT}\right) \qquad (1)$$

where P_0 is the barometric pressure measure at the MeteoSwiss station (mbar), h_0 and h (m) are the altitude of the meteorological and at the monitoring stations, respectively, g is the gravity acceleration (9.81 m s^{-2}), M the molar mass of air (0.0289644 kg mol^{-1}), R the universal gas constant (8.31432 J m mol^{-1} K^{-1}). The temperature of air T_{air} (°C) at the METALP stations is estimated through the temperature T_0 (°C) measured at the MeteoSwiss station (equation 2), where the temperature gradient ΔT/ Δh is set to 0.54 °C/100.

$$T_{air} = T_0 - \left((h - h_0) \cdot \frac{\Delta T}{\Delta h}\right) \qquad (2)$$

Measured concentrations of pCO_2 (ppm) were adjusted to site-specific conditions following the manufacturer's suggested equation:

$$pCO_{2,corr} = pCO_2 \cdot \frac{p}{1013} \cdot \frac{298}{273.15 + T_W} \qquad (3)$$

where *p* (mbar) corresponds to the barometric pressure at location and T_w (°C) the water temperature. Dissolved CO_2 concentration (µmol L^{-1}) was then derived by multiplying the corrected $pCO_{2,corr}$ with Henry's constant K_H (mol L^{-1} atm^{-1}) and with the barometric pressure, p (atm), at each site:

$$[CO_2] = pCO_{2,corr} \cdot K_H \cdot p \qquad (4)$$

K_H is a function of water temperature (T_k, K) with A is 108.3865, B is 0.01985076, C is -6919.53, D is -40.4515, E is 669365 according to Plummer and Busenberg (1982).

$$K_H = 10^{A + B \cdot T_K + \frac{C}{T_K} + D \cdot \log_{10}(T_K) + \frac{E}{T_K^2}} \qquad (5)$$

The standard gas transfer velocity (k_{600}, m d^{-1}) was calculated using the relationships proposed by Ulseth et al. (2019) for high-energy streams:

$$\ln(k_{600}) \text{ for } eD > 0.02 = 1.18 \cdot \ln(eD) + 6.63 \qquad (6)$$

$$\ln(k_{600}) \text{ for } eD < 0.02 = 0.35 \cdot \ln(eD) + 3.10 \qquad (7)$$

where eD is the stream energy dissipation rate (m^2 s^{-3}), which is obtained by multiplying the gravity acceleration with slope (S, unitless) and stream flow velocity (v, m s^{-1})

$$eD = g \cdot S \cdot v \qquad (8)$$

Velocity was calculated with discharge ($m^3\ s^{-2}$) according to the hydraulic geometry scaling proposed by Horgby et al. (2019):

$$v = 0.668 \cdot Q^{0.365} \qquad (9)$$

To convert k_{600} to k_{CO2} (equation 11) we used the temperature dependent Schmidt scaling according to Wanninkhof (2014)

$$Sc_{CO_2} = 1923.6 - 125.06 \cdot T_W + 4.3773 \cdot T_W^2 - 0.85681 \cdot T_W^3 + 0.00070284 \cdot T_W^4 \qquad (10)$$

$$k_{CO_2} = \frac{k_{600}}{\left(\frac{600}{Sc_{CO_2}}\right)^{-0.5}} \qquad (11)$$

The flux was finally calculated using the following relationship

$$F_{CO_2} = k_{CO_2} \cdot \Delta CO_2 \qquad (12)$$

were ΔCO_2 (g CO_2-C L^{-1}) represent the gradient between the measured concentration of stream-water CO_2 ($CO_{2,water}$) and the equilibrium concentration ($CO_{2,sat}$).

The equilibrium CO_2 concentration (µmol L^{-1}) was calculated using monthly mean atmospheric CO_2 measured at the Jungfraujoch, the ratio between of atmospheric pressure at a site (P_{atm}, atm) and standard pressure of 1 atmosphere (P_{std}, atm) and Henry's Law constant for CO_2 (K_H):

$$[CO_{2,sat}] = CO_{2,Jungfrau} \cdot \frac{P_{atm}}{P_{std}} \cdot K_H \qquad (13)$$

1.3 Data analysis

All data processing and analysis was performed with the software environment for statistical computing and graphics R (version 4.1.2). We investigated possible influences on median CO_2 concentration by exploring the correlation with various watershed and stream characteristics, including glacial coverage, vegetation coverage, slope, catchment average slope, altitude, temperature, and discharge. The Pearson's correlation coefficient (r) was calculated to measure these relationships. To determine differences between median concentrations between catchments, we used the Kruskall-Wallis test. For all statistical analyses, a significance level of $\alpha = 0.05$ was used.

We followed the approach used by Liu and Raymond (2018) to assess the responsiveness of CO_2 concentration and flux to discharge regimes. From the high-frequency data, we found the median daily values of specific discharge (q, mm d^{-1}), CO_2 concentration, and CO_2 flux. We then determined the slope of the power law function to analyse the magnitude and the typology of response of CO_2 concentration and CO_2 flux to specific discharge. A C-q slope of zero, or near-zero, is commonly interpreted as chemostatic behaviour, where chemical concentrations remain relatively constant as discharge varies. Here we define a C-q slope as chemostatic if the slope is between −0.2 and +0.2. Whether slopes of less than -0.2 were considered sour limitation, and slopes greater than 0.2 were considered transport limitation (Godsey et al. 2009).

Results

Hydrological regimes and stream water CO_2 concentration dynamics

Table 2: Median CO_2 concentration, CO_2 saturation, gas exchange, and CO_2 flux at the twelve monitored sites. The interquartile range is shown in parentheses.

Site	Median CO_2 concentration (µmol L^{-1})	CO_2 saturation (%)	Median k_{600} (m d^{-1})	Median CO_2 flux (g C d^{-1} m^{-2})
VAD	17.0 (4.7)	78.6 (12.9)	398 (500)	-21.7 (29.5)
VAU	15.1 (5.19)	67.3 (16.7)	202 (200)	-11.4 (20.3)
VEL	16.2 (5.97)	77.8 (26)	31.2 (42.1)	-1.54 (2.06)
FED	21.5 (8.43)	94.1 (30.9)	86.3 (21.7)	-0.894 (5.12)
FEU	30.4 (23.4)	148 (82.8)	118 (59.5)	6.01 (14.6)
PEU	18.7 (4.37)	96.3 (21.1)	76.7 (28.5)	-0.4 (2.97)
AND	23.6 (2.96)	98.8 (6.01)	467 (138)	-1.05 (4.93)
ANU	27.6 (5.82)	124 (24.1)	75.6 (69.8)	3.86 (7.51)
RIC	23.2 (2.42)	100 (8.97)	183 (149)	-0.113 (2.22)
VID	29.4 (14.1)	127 (73)	204 (104)	11.2 (18.1)
VIM	20.1 (6.68)	96.6 (21.2)	146 (82)	-0.842 (8.02)
VIU	23.3 (15.4)	108 (67.5)	34.5 (11.6)	0.453 (2.48)

Across all study sites, median concentration of CO_2 ranged from 15.1 µmol L^{-1} at VAU to 30.4 µmol L^{-1} at FEU (Table 2). This represents a percent saturation of 69.3% to 140.7%, respectively (Figure 2). Over the entire monitoring period, six sites exhibited median CO_2 concentrations below saturation (VAD, VAU, VEL, FED, PEU, VIM), and six sites above saturation (FEU, AND, ANU, RIC, VID, VIU). At two sites, VAU and VAD, the dissolved concentration of CO_2 was almost always below saturation (Table 2). At all other sites, CO_2 concentrations below and above saturation were observed. At VID, the CO_2 concentration was below saturation only 9.0% of the monitored period, the least of any

EPFL

site. The minimum instantaneous CO_2 concentration was 2.5 µmol L^{-1} at VAU, while the highest concentration was 68.3 µmol L^{-1} at VID. The interquartile range of concentrations observed at a site was always lower than the median concentration, suggesting that temporal variation in concentration is relatively limited.

Regarding calculated standard gas transfer velocities (k_{600}) AND showed the highest median value with 467 m d^{-1}, while VEL had the lowest median value with 31.2 m d^{-1} (Table 2). VAD had widely the largest variability in k_{600} between sites (IQR=500), while VIU the lowest (IQR = 11.6).

The lowest and highest median CO_2 flux values were found at VAD (-21.7 g C-CO_2 d^{-1} m^{-2}) and VID (11.2 g C-CO_2 d^{-1} m^{-2}), respectively (Table 2). Following the patterns in CO_2 saturation, six streams (VAD, VAU, VEL, FED, PEU, VIM), exhibited median rates of CO_2 influx over the study period while the remaining streams exhibited efflux (FEU, AND, ANU, RIC, VID, VIU). Instantaneous CO_2 fluxes ranged from -130 g C-CO_2 d^{-1} m^{-2} at VAD to 129 VID g C-CO_2 d^{-1} m^{-2}. VAD showed the highest variability in flux (IQR = 29.5 g C-CO_2 d^{-1} m^{-2}) and VEL the lowest (IQR = 2.06 g C-CO_2 d^{-1} m^{-2}). Differences in median annual CO_2 flux were observed, with some sites experiencing years of overall influx and others of overall efflux. For example, the median flux at FED in 2019 was -1.11 g C-CO_2 d^{-1} m^{-2} and in 2020 was 4.85 g C-CO_2 d^{-1} m^{-2}.

We measured relatively low DOC concentrations (< 400 µg L^{-1}) across all catchments. The Champéry catchment had the highest median DOC concentration (375 µg L^{-1}; $p < 0.01$). Other catchments had similar concentrations with median values ranging from 149 µg L^{-1} at Ferret to 215 µg L^{-1} at Valsorey. δ^{13}C-DIC was depleted in our streams relative to atmospheric equilibrium with median values ranging between -5.95‰ at Valsorey to -9.28‰ at Champéry. Again, Champéry was significantly difference compared to the other catchments ($p < 0.01$). The median concentration of CO_2 most strongly correlated to site elevation ($r = -0.53$), temperature ($r = 0.43$), watershed glacial coverage ($r = -0.43$), and watershed vegetation coverage ($r = 0.42$). All other variables exhibited correlations below 0.30.

We observed O_2 percent saturation to be relatively uniform compared to CO_2, both spatially and temporally. All sites were typically close to saturation or slightly undersaturated, with median values ranging from 94.8% at VEL to 99.7% at AND (Table S1). Variability in CO_2 saturation was much greater than O_2, with the minimum difference between the 5th and 95th percentiles being approximately 20% for CO_2 and the maximum difference being approximately 10% for O_2.

Inverse relationships between CO_2 concentration and specific discharge were most). The median value for the parameter b_c was -0.10 and ranged between -0.37 at FEU to 0.03 at VEL common (Table S2). Every site can be defined as chemostatic, with the sole exception of FEU which showed source limitation dynamics ($b_c = -0.37$) (Figure S7). Ten of the sites exhibited significant ($p < 0.05$) C-q relationships, with the exception of FED and VIM. For CO_2 flux, the median value of b_F was -0.01 ranging between -0.14 at VAD and 0.03 at AND (Figure S8). Again, all sites are defined as chemostatic. Here, all sites exhibited significant relationships, except for VIM.

Figure 2: Time series of daily median CO_2 saturation across the twelve monitored streams. The dashed line represents 100% saturation, and point above the line denote supersaturation

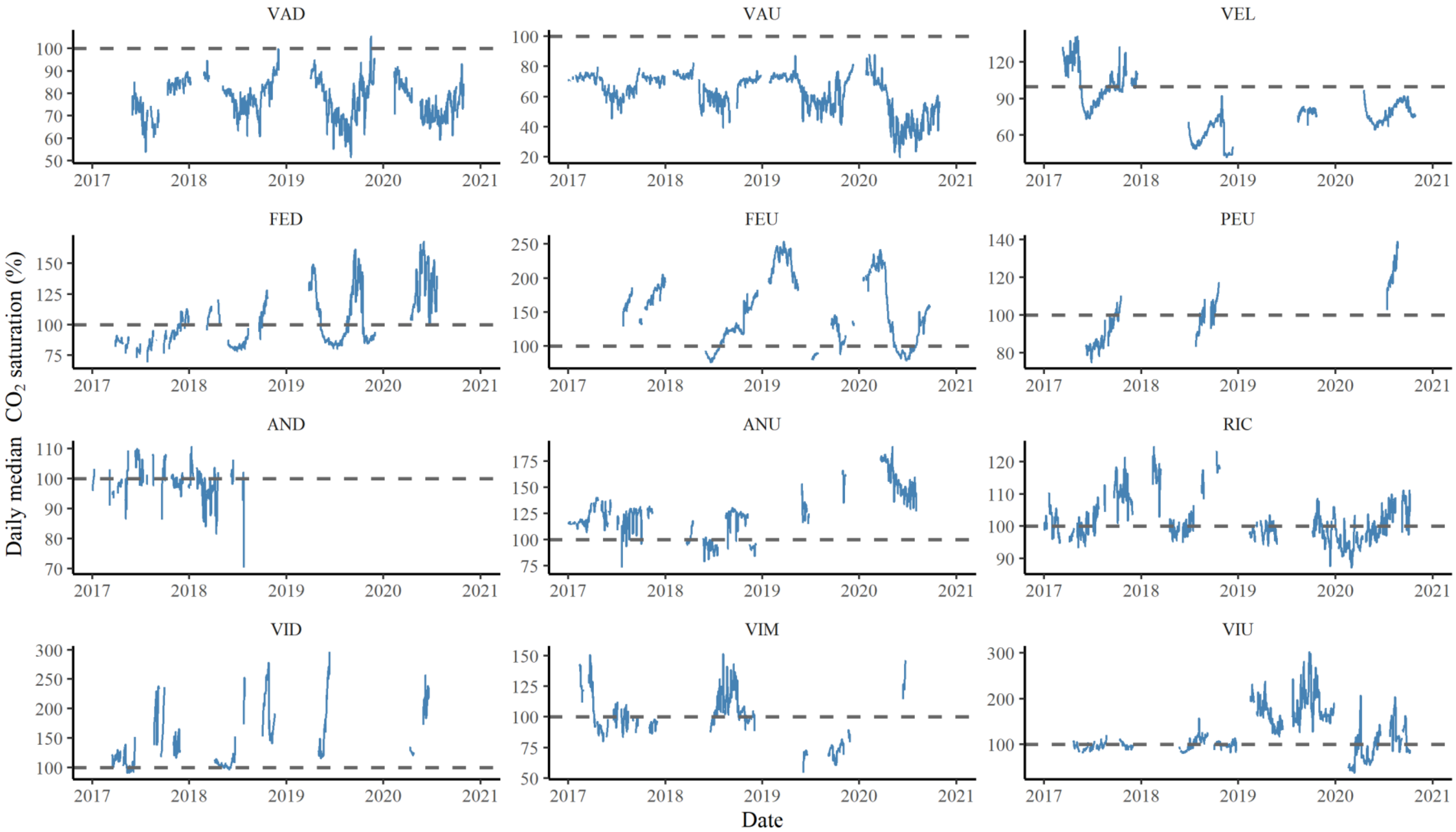

Discussion

Alpine streams can be sinks of CO_2

The streams in this study were found to be both sources and sinks of CO_2 to the atmosphere. Globally, streams have most often been found to be sources of CO_2 to the atmosphere (Raymond et al. 2013). Exceptions to this general pattern have been found where in-stream photosynthesis is high (Pu et al. 2017), or where weathering within the catchment and stream acts as a sink of CO_2(Clark and Fritz 1997). Specifically, streams draining glaciers in Canada were shown to be significant sinks of CO_2 as a result of the influence of weathering reactions (St. Pierre et al. 2019). Decomposition and CO_2 production in these environments is low because of relatively low inputs of terrestrial organic carbon, as a result, weathering subsequent from the erosion of poorly consolidated landscapes, typical of glacierized catchments, dominates the CO_2 balance. Indeed, the streams in this study with the highest glacier influence (VAU and VAD) were the largest sinks of CO_2. This concept is sustained additionally by the negative relationship we found between the CO_2 concentration and glaciated coverage. Nevertheless, we found that most sites that are not glacier-fed were prone to be undersaturated in CO_2 during at least some periods, making them even relevant unexpected sinks. It becomes therefore essential to understand the mechanisms that make these streams absorb CO_2 from the atmosphere likewise the glacier-fed freshwater ecosystem. Carbon isotopes measurements provide useful insight about processes influencing this behaviour (Clark and Fritz 1997). In fact, δ^{13}C-DIC in all our study streams, glacier-fed and not, was highly depleted relative to atmospheric equilibrium. The only processes that could have led to depletion in δ^{13}C-DIC are weathering and oxidation of organic carbon. However, dissolved organic carbon concentrations found in our study site were relatively negligible to justify oxidation as the main driver of δ^{13}C-DIC depletion. Furthermore, organic carbon consumption would have resulted in oversaturation of co2, not in undersaturation as observed in our study.

That is, we observe glacier-influenced streams that are sources of CO_2 (e.g., FEU, ANU) and streams without glacier influence that are sinks of CO_2 (e.g., VEL, PEU). As a result, whether a stream in our study is a sink or a source of CO_2 must depend on additional factors, and that weathering may be relevant in high elevation catchments more broadly than glacier-influenced ones only**.** Photosynthesis may play a small role in reducing CO_2 concentrations in these streams, but it is likely minimal when compared to weathering. Rates of gross primary productivity (GPP) have been estimated in these streams previously (Boix Canadell et al. 2021). Rates, measured during optimal conditions for GPP, were generally less than 2 g O_2 m^{-2} d^{-1}. Given the influx of CO_2 to these streams routinely exceeds 2 g CO_2 m^2 d^{-1}, photosynthesis could not account for this alone. Similarly, the saturation of O_2

in these streams is typically near saturation or below (Table S1). If photosynthesis was significant, we would expect O_2 saturation to be elevated above saturation. Thus, while in-stream GPP is likely occurring and acting as a small sink of CO_2, we expect the majority of CO_2 undersaturation is explained by weathering in the catchment and stream.

Sources of CO_2 limited in montane catchments

Weathering is occurring in all of these catchments, so the determination of whether a site is a sink or source of CO_2 is also dependent on the relative amount of CO_2 sources. Sources of CO_2 to a stream can be internal, from the processing of organic matter, or external, typically from the transport of soil respiration via groundwater to the stream (Hotchkiss et al. 2015). In small streams generally, external sources have been shown to be most important. However, in the high elevation catchments, soils are typically very thin and little developed (Egli et al. 2006). Typically, soil depth decreases with elevation, with little to no soil development at very high elevations.

Another possible source of CO_2 could be in-stream decomposition of organic matter. This is a mechanism that is likely occurring in the sites. However, Boix Canadell et al. (2021) found low respiration rates in our study streams. Furthermore, our results suggest we can exclude oxidation of organic carbon in stream to be a relevant process. We found relatively low concentrations of DOC in all our streams, as well as O_2 concentrations close to saturation (Table 1). These data suggest that there are not substantial amounts of organic carbon that could potentially be converted to CO_2, and that O_2 is not consumed considerably by biological mechanisms, excluding the contribution of processing of organic carbon to be a relevant CO_2 source.

Influence of discharge on CO_2 sources, concentration, and emissions

The C-q relationships we found across our sites were chemostatic, suggesting that the main processes that we defined in the catchments, namely weathering and soil respiration, are not clearly transport or source limited. VAD and VAU tend to be more source limited than other sites. Since these are the streams draining the biggest glaciers, this result suggests a higher rate of weathering for highest discharges, consequently of the action of meltwaters transporting reactive sediments highly affected by weathering. C-q relationships furnish interesting insights about CO_2 transports across the watersheds, however the unexpected tendency of our study sites to be sinks of CO_2 make complicated to interpret the results. When in-stream CO_2 concentration is below saturation, the atmosphere acts as an additional source of CO_2, complicating the assumptions of source location within the watershed for C-q analysis.

While glaciers may be indicative of higher potential rates of weathering, our results suggest that the presence of glaciers is of itself not determinate of whether a stream is a sink or source of CO_2. As stated above multiple factors indicate at weathering as a main process occurring in all our catchments. However, CO_2 consumed by this process is balanced by the CO_2 produced by organic matter within the catchment, as a consequence, the final tendency for a stream to act as a net source or sink of CO_2 depends mostly on the terrestrial carbon delivered to the stream. In this regard, it is of particular interest how Guelland et al. (2013) demonstrated how respiration increases with soil development. An important increase of rates of CO_2 effluxes has been shown to be linked with soil carbon accumulation and vegetation cover. Our results confirm this pattern as we found a positive relationship between CO_2 concentration and vegetation coverage. We therefore suggest that soil development can be a key factor to determine the CO_2 metabolism of high mountain streams.

Conclusion

Overall, our study confirms pervious finding regarding glacier-fed streams being significant CO_2 sinks. However, our results suggest that high mountain streams without a glacier can be overlooked CO_2 sinks due to weathering being in some cases the predominant process. We suggest that variation in terrestrial respiration across different type of catchments is a determining factor to the net tendency of freshwater ecosystem to either outgas or absorb CO_2.

Further analysis on soil properties, such as composition, chemistry and development, in our study catchments could help to further describe the relationships between in stream CO_2 fluxes and watersheds spatial attributes. This approach could in particular be useful to better assess and characterize the main processes occurring in high mountain streams, allowing to further comprehend mechanisms driving CO_2 dynamics.

EPFL

Acknowledgements

Firstly, I would like to thank Andrew Lean Robinson and Nicola Deluigi for the outstanding quality of supervising of my master project. Their support and advice have been fundamental to face the different challenges that this work needed.

I would also like to thank Professor Tom Battin for allowing me to carry out my Master's project in the River ecosystem laboratory.

References

Battin, T. J., S. Luyssaert, L. A. Kaplan, A. K. Aufdenkampe, A. Richter, and L. J. Tranvik. 2009. The boundless carbon cycle. Nature Geosci **2**: 598–600. doi:10.1038/ngeo618

Boix Canadell, M., L. Gómez-Gener, A. J. Ulseth, M. Clémençon, S. N. Lane, and T. J. Battin. 2021. Regimes of primary production and their drivers in Alpine streams. Freshwater Biology **66**: 1449–1463. doi:10.1111/fwb.13730

Canadell, M. B., L. Gómez-Gener, M. Clémençon, S. N. Lane, and T. J. Battin. 2021. Daily entropy of dissolved oxygen reveals different energetic regimes and drivers among high-mountain stream types. Limnology and Oceanography **66**: 1594–1610. doi:10.1002/lno.11670

Clark, I. D., and P. Fritz. 1997. Environmental Isotopes in Hydrogeology, CRC Press.

Clow, D. W., R. G. Striegl, and M. M. Dornblaser. 2021. Spatiotemporal Dynamics of CO_2 Gas Exchange From Headwater Mountain Streams. J Geophys Res Biogeosci **126**. doi:10.1029/2021JG006509

Diamond, J. S., and M. J. Cohen. 2018. Complex patterns of catchment solute–discharge relationships for coastal plain rivers. Hydrological Processes **32**: 388–401. doi:10.1002/hyp.11424

Drake, T. W., P. A. Raymond, and R. G. M. Spencer. 2018. Terrestrial carbon inputs to inland waters: A current synthesis of estimates and uncertainty. Limnology and Oceanography Letters **3**: 132–142. doi:10.1002/lol2.10055

Egli, M., M. Wernli, C. Kneisel, and W. Haeberli. 2006. Melting Glaciers and Soil Development in the Proglacial Area Morteratsch (Swiss Alps): I. Soil Type Chronosequence. Arctic, Antarctic, and Alpine Research **38**: 499–509. doi:10.1657/1523-0430(2006)38[499:MGASDI]2.0.CO;2

Godsey, S. E., J. W. Kirchner, and D. W. Clow. 2009. Concentration–discharge relationships reflect chemostatic characteristics of US catchments. Hydrological Processes **23**: 1844–1864. doi:10.1002/hyp.7315

Guelland, K., F. Hagedorn, R. H. Smittenberg, H. Göransson, S. M. Bernasconi, I. Hajdas, and R. Kretzschmar. 2013. Evolution of carbon fluxes during initial soil formation along the forefield of Damma glacier, Switzerland. Biogeochemistry **113**: 545–561. doi:10.1007/s10533-012-9785-1

Horgby, Å., L. Gómez-Gener, N. Escoffier, and T. J. Battin. 2019. Dynamics and potential drivers of CO_2 concentration and evasion across temporal scales in high-alpine streams. Environ. Res. Lett. **14**: 124082. doi:10.1088/1748-9326/ab5cb8

Hotchkiss, E. R., R. O. Hall Jr, R. A. Sponseller, D. Butman, J. Klaminder, H. Laudon, M. Rosvall, and J. Karlsson. 2015. Sources of and processes controlling CO2 emissions change with the size of streams and rivers. Nature Geosci **8**: 696–699. doi:10.1038/ngeo2507

Johnson, M. S., M. F. Billett, K. J. Dinsmore, M. Wallin, K. E. Dyson, and R. S. Jassal. 2010. Direct and continuous measurement of dissolved carbon dioxide in freshwater aquatic systems—method and applications. Ecohydrology **3**: 68–78. doi:10.1002/eco.95

Johnson, M. S., J. Lehmann, S. J. Riha, A. V. Krusche, J. E. Richey, J. P. H. B. Ometto, and E. G. Couto. 2008. CO2 efflux from Amazonian headwater streams represents a significant fate for deep soil respiration. Geophysical Research Letters **35**. doi:10.1029/2008GL034619

Lauerwald, R., G. G. Laruelle, J. Hartmann, P. Ciais, and P. A. G. Regnier. 2015. Spatial patterns in CO2 evasion from the global river network. Global Biogeochemical Cycles **29**: 534–554. doi:10.1002/2014GB004941

Liu, S., and P. A. Raymond. 2018. Hydrologic controls on *pCO* $_2$ and CO $_2$ efflux in US streams and rivers: Hydrologic controls on river CO $_2$ efflux. Limnol. Oceanogr. **3**: 428–435. doi:10.1002/lol2.10095

Marx, A., J. Dusek, J. Jankovec, M. Sanda, T. Vogel, R. van Geldern, J. Hartmann, and J. a. C. Barth. 2017. A review of CO2 and associated carbon dynamics in headwater streams: A global perspective. Reviews of Geophysics **55**: 560–585. doi:10.1002/2016RG000547

Meybeck, M., P. Green, and C. Vörösmarty. 2001. A New Typology for Mountains and Other Relief Classes: An Application to Global Continental Water Resources and Population Distribution. Mountain Research and Development - MT RES DEV **21**: 34–45.

Plummer, L. N., and E. Busenberg. 1982. The solubilities of calcite, aragonite and vaterite in CO2-H2O solutions between 0 and 90°C, and an evaluation of the aqueous model for the system CaCO3-CO2-H2O. Geochimica et Cosmochimica Acta **46**: 1011–1040. doi:10.1016/0016-7037(82)90056-4

Pu, J., J. Li, M. B. Khadka, J. B. Martin, T. Zhang, S. Yu, and D. Yuan. 2017. In-stream metabolism and atmospheric carbon sequestration in a groundwater-fed karst stream. Science of The Total Environment **579**: 1343–1355. doi:10.1016/j.scitotenv.2016.11.132

Schlesinger, W. H., and J. A. Andrews. 2000. Soil respiration and the global carbon cycle. Biogeochemistry **48**: 7–20. doi:10.1023/A:1006247623877

St. Pierre, K. A., V. L. St. Louis, S. L. Schiff, I. Lehnherr, P. G. Dainard, A. S. Gardner, P. J. K. Aukes, and M. J. Sharp. 2019. Proglacial freshwaters are significant and previously unrecognized sinks of atmospheric CO $_2$. Proc Natl Acad Sci USA **116**: 17690–17695. doi:10.1073/pnas.1904241116

Ulseth, A. J., R. O. Hall, M. Boix Canadell, H. L. Madinger, A. Niayifar, and T. J. Battin. 2019. Distinct air–water gas exchange regimes in low- and high-energy streams. Nat. Geosci. **12**: 259–263. doi:10.1038/s41561-019-0324-8

Wallin, M. B., T. Grabs, I. Buffam, H. Laudon, A. Ågren, M. G. Öquist, and K. Bishop. 2013. Evasion of CO2 from streams – The dominant component of the carbon export through the aquatic conduit in a boreal landscape. Global Change Biology **19**: 785–797. doi:10.1111/gcb.12083

Wanninkhof, R. 2014. Relationship between wind speed and gas exchange over the ocean revisited. Limnology and Oceanography: Methods **12**: 351–362. doi:10.4319/lom.2014.12.351

Supplementary information to:

High mountain streams could act as sources or sinks of CO_2 depending on watersheds characteristics

Table S1: The median percent saturation of dissolved oxygen (O_2) and carbon dioxide (CO_2) at the twelve sites from all instantaneous sensor measurements. The 5th and 95th percentiles are shown in parentheses.

Site	**O_2**		**CO_2**	
VAD	98.2	(96.8, 102.7)	79.1	(64.0, 93.9)
VAU	98.4	(96.1, 103.9)	69.3	(37.5, 78.8)
VEL	94.8	(92.3, 98.4)	80.1	(46.4, 122.5)
FED	97.2	(93.9, 99.4)	92.9	(80.4, 155.8)
FEU	96.9	(93.7, 99.4)	140.7	(74.7, 246.8)
PEU	97.0	(94.7, 100.0)	96.7	(80.1, 127.1)
AND	99.7	(96.3, 101.3)	100.5	(90.4, 110.4)
ANU	96.7	(93.1, 99.6)	125.0	(93.7, 180.0)
RIC	97.8	(94.4, 99.6)	102.7	(94.9, 118.9)
VID	97.4	(89.4, 100.0)	133.6	(99.5, 249.3)
VIU	96.8	(93.8, 99.4)	105.1	(68.4, 214.1)
VIM	98.7	(96.8, 101.1)	97.3	(70.4, 133.5)

Figure S1: Time series of daily median CO_2 concentration across the twelve monitored streams.

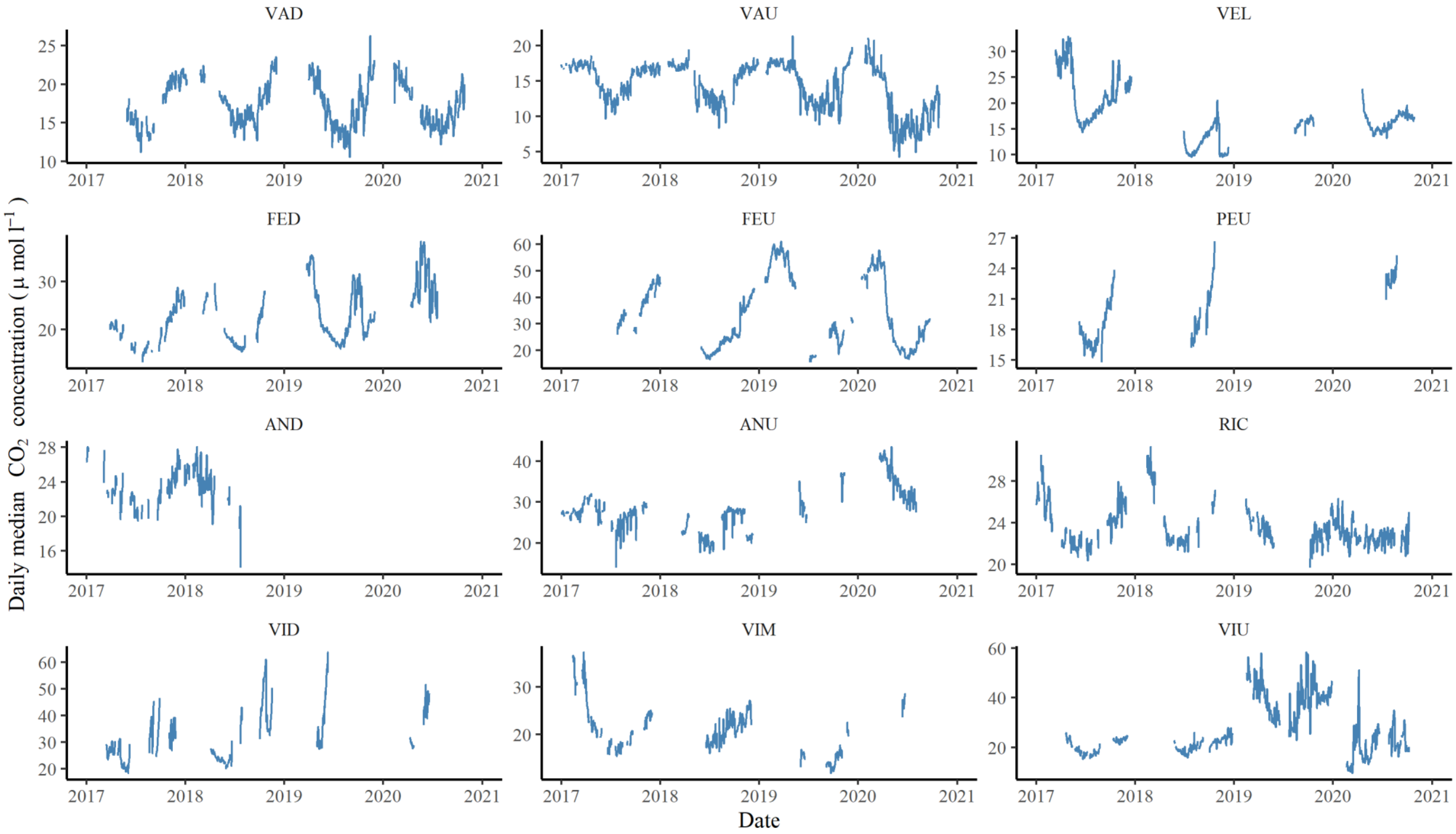

EPFL

Figure S2: Time series of k_{600} across the twelve monitored streams.

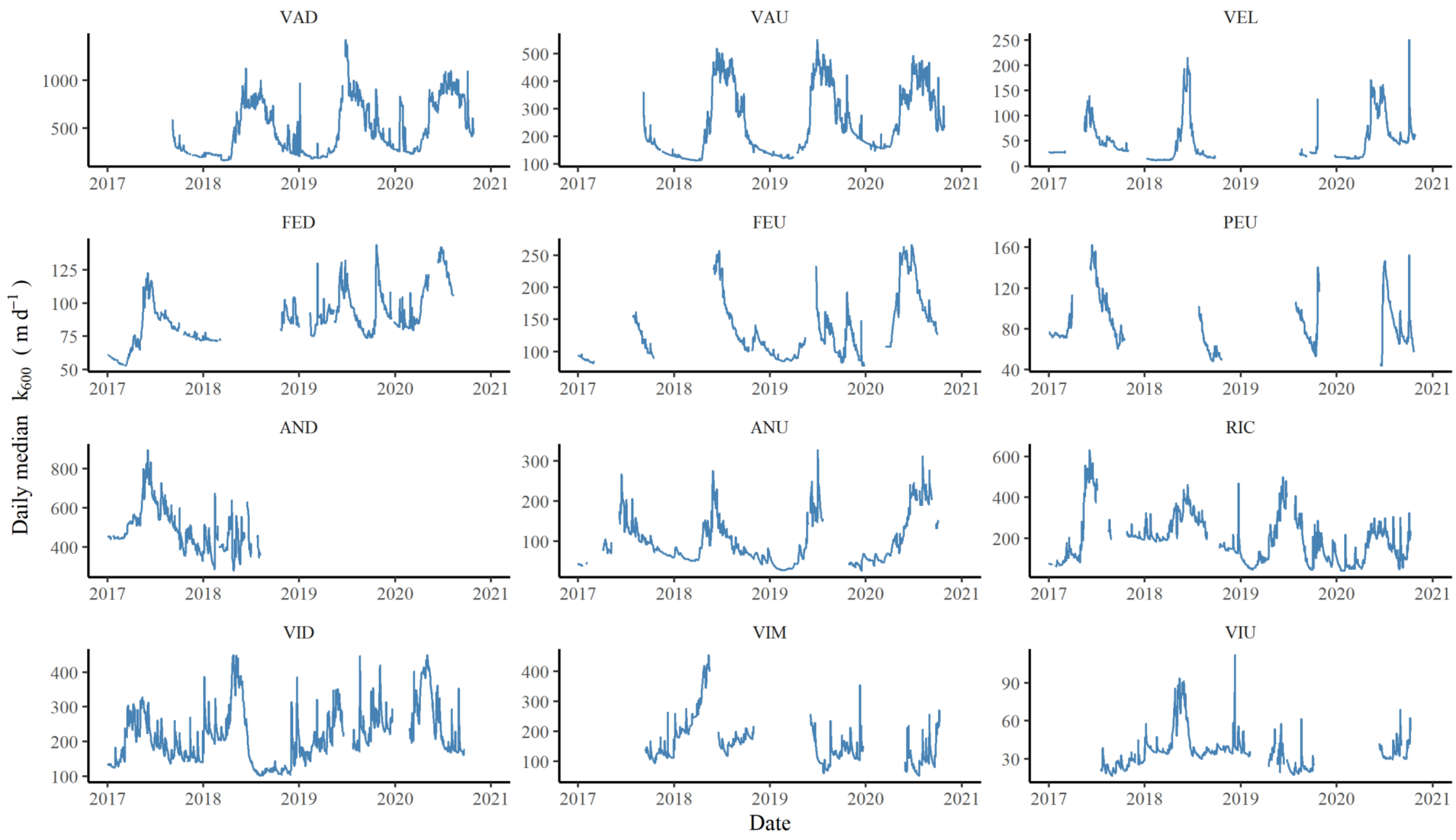

EPFL

Figure S3: Time series of daily median CO_2 flux across the twelve monitored streams.

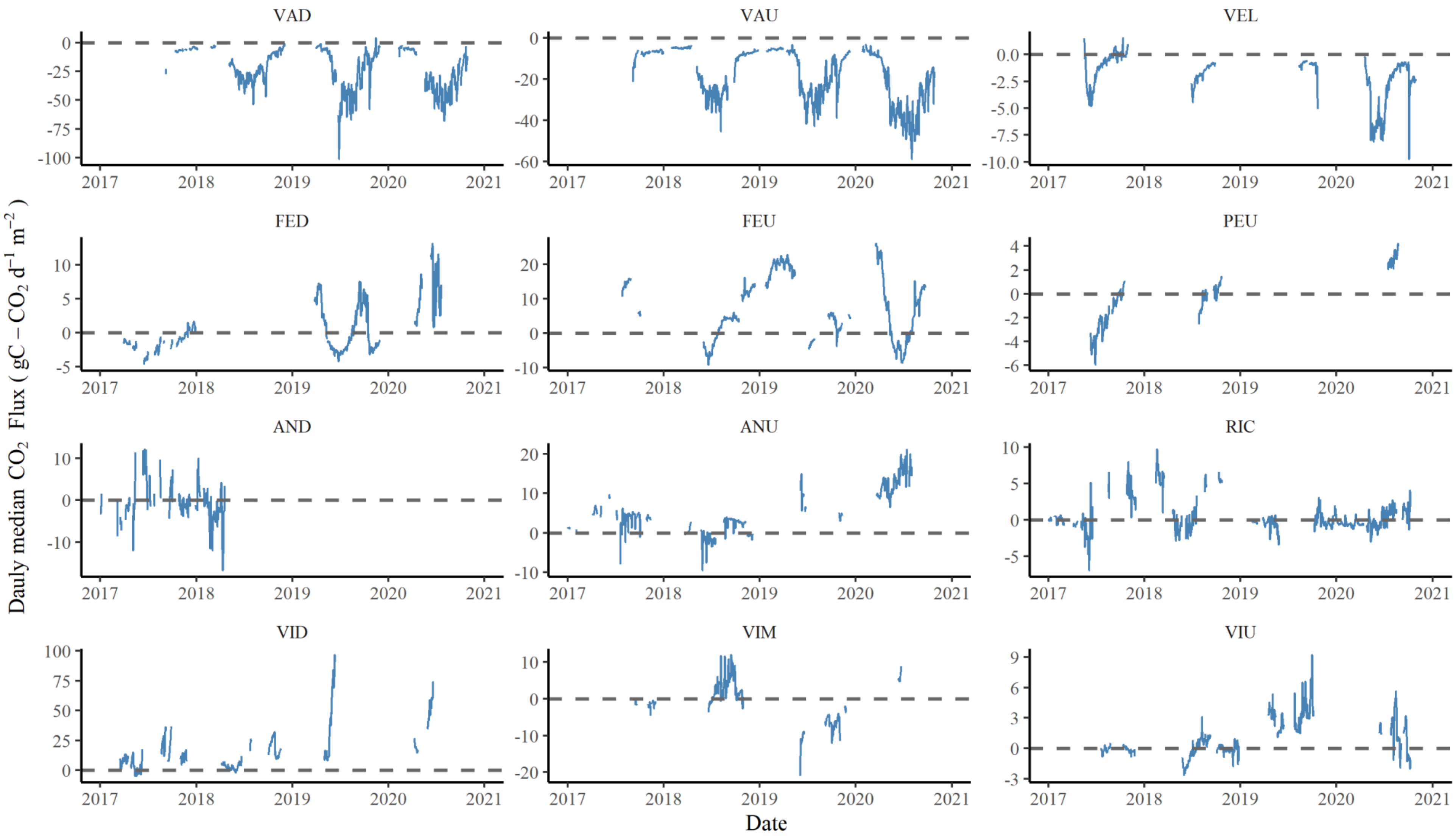

Table S2: Power slopes of the linear regressions for daily median CO_2 concentration versus daily median runoff (b_C), and daily median F_{CO2} versus daily median runoff (b_F). Flux data was log 10 transformed prior to analysis (x+120) to keep potential negative CO_2 evasion fluxes.

		CO_2 vs. specific discharge			**F_{CO2} vs. specific discharge**		
Site	**n**	**b_c**	**R^2**	**P-value**	**b_F**	**R^2**	**P-value**
VAD	783	-0.11	0.72	<0.01	-0.14	0.71	<0.01
VAU	1006	-0.19	0.56	<0.01	-0.10	0.78	<0.01
VEL	532	0.03	0.04	<0.01	-0.01	0.56	<0.01
FED	493	-0.02	0.00	0.27	0.01	0.01	0.03
FEU	644	-0.37	0.55	<0.01	-0.07	0.53	<0.01
PEU	238	-0.11	0.32	<0.01	-0.02	0.37	<0.01
AND	247	-0.10	0.33	<0.01	0.03	0.12	<0.01
ANU	515	-0.02	0.01	<0.01	0.02	0.15	<0.01
RIC	723	-0.01	0.05	<0.01	0.00	0.01	0.04
VID	359	-0.16	0.29	<0.01	-0.02	0.02	<0.01
VIM	268	0.00	0.00	0.91	-0.01	0.01	0.10
VIU	497	-0.12	0.11	<0.01	-0.01	0.21	<0.01

Figure S7: Relationship between streamwater CO_2 concentration and specific discharge for each study site.

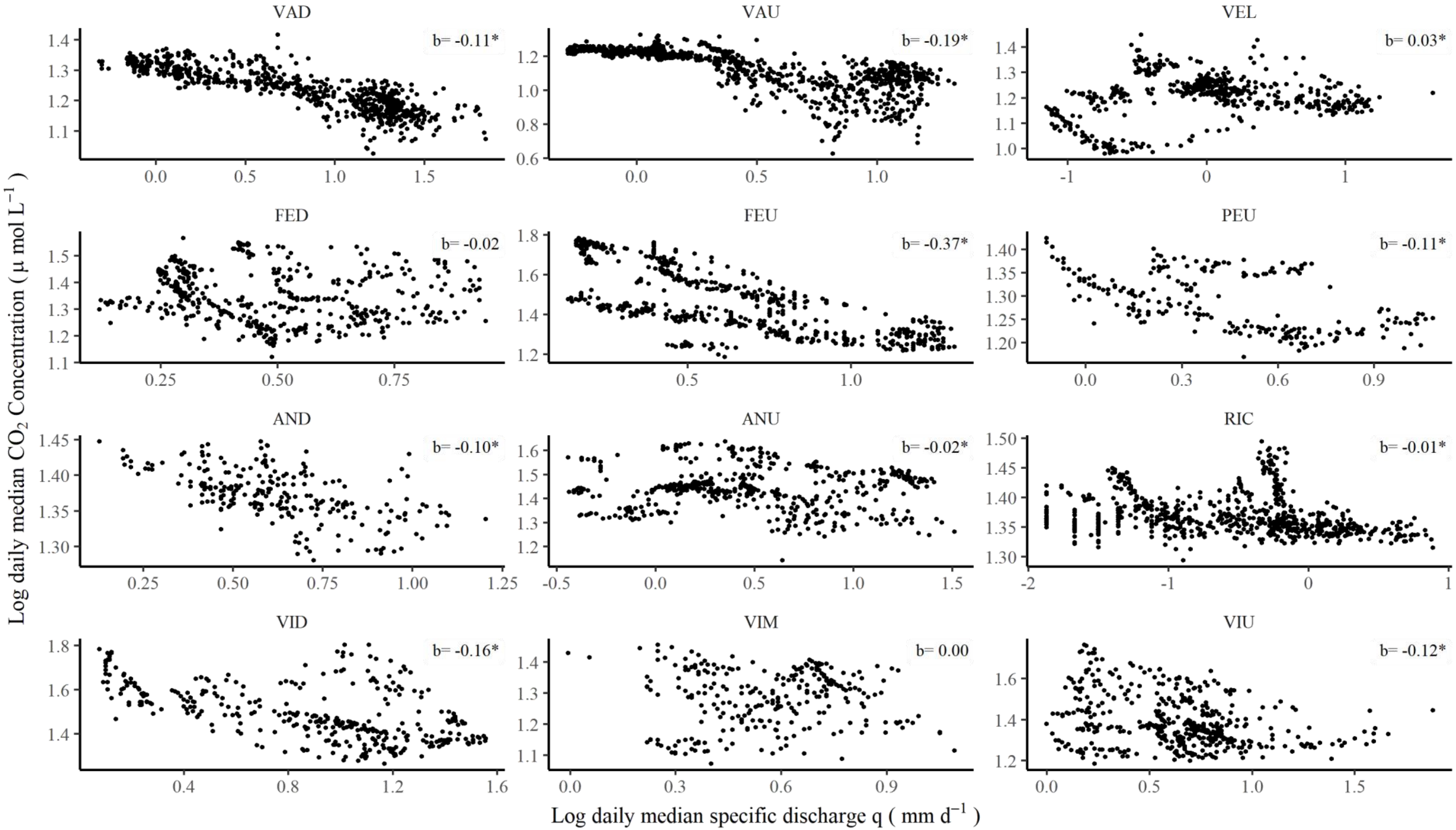

Figure S8: Relationship between streamwater CO_2 fluxes to specific discharge for each study site